ASSESSING THE FEASIBILITY OF SOLAR ABSORPTION COOLING FOR CANADIAN HOUSING

Courtney L. Edwards, Ian Beausoleil-Morrison, Cynthia A. Cruickshank, and Geoffrey Johnson

Department of Mechanical and Aerospace Engineering, Carleton University, Ottawa (Canada)

1. Introduction

Residential energy demand from space-cooling in Canada has increased by over 200% in the last twenty years (NRCan, 2008). Presently, the most common space-cooling technology in use is electrically driven vapour compression systems. These systems place a large strain on the central electricity system during the summer months, and in Ontario, Canada, these large loads are typically powered by non-renewable sources of energy. Across Canada, space-cooling resulted in the emission of 1.2 Mt of CO_2 equivalent (CO_{2e}) in 2008, with 1.0 Mt resulting from central systems. While improvements are being realized in the thermal envelope of households, space-cooling remains a significant component of residential energy use in the summer months during peak periods of electrical demand.

As an alternative, solar power can be used as an energy source in a residential space-cooling system, removing the bulk of the energy demand of the system from the electricity grid. The addition of this renewable energy source reduces the peak summer loads on the electrical grid, and therefore decreases the GHG contributions from cooling systems.

1.1 Solar Absorption Cooling

Solar absorption cooling (SAC) utilizes solar energy and harmless working fluids (refrigerants) such as water, to produce chilled fluid for the removal of heat through space-cooling (Balghouthi et al., 2005). The typical COP_{th} of a single-effect absorption system is 0.5-0.8 (Henning, 2007).

In 2003, the Solar Air Conditioning in Europe Project investigated 54 solar cooling projects across Europe. This research has shown solar cooling to result in primary energy savings of 40-50% (Balaras et al., 2007). However, solar insolation fluctuates considerably with latitude, and studies have shown that climate is a strong factor in the performance of solar cooling systems (Mateus & Oliviera, 2009). Research investigating the viability of solar cooling systems in a Canadian climate is scarce, and consequently there is a need for studies for Canadian applications. In addition, while much research has been completed in the area of building space-cooling, for example for the Shanghai Institute of Building Science in China (Zhai & Wang, 2009), research concerning the application of solar cooling in residential housing has been less prevalent.

1.2 Research Objectives

In order to assess the feasibility of SAC for Ontario houses, the design, commissioning, and testing of an absorption chiller were undertaken (Johnson, 2011). This experimental work focused on gathering reliable experimental performance data to calibrate a model of an absorption chiller suitable for building performance simulation. Following the experimental work, appropriate control schemes for a residential SAC system were established. Initial simulations of the SAC system were conducted to dimension system components using TRNSYS simulation software. The existing thermal air conditioning model in the ESP-r simulation environment was then calibrated and refined using the experimental data. A complete SAC system in ESP-r was developed using the refined thermal air conditioning model and other appropriate system components for simulation within models of representative Ontario houses. Finally, an assessment of the SAC system in houses with different operating conditions and for different climatic regions was performed. The viability of the system was determined based on the energy and greenhouse gas performance of the system.

2. Experimental Setup

A test facility was designed and assembled to experimentally characterize the performance of a Yazaki WFC-SC10 (35 kW) lithium/bromide absorption chiller (Aroace, 2010) under different steady-state operating boundary conditions. The purpose of the absorption chiller test facility was to gather performance

data for a range of heat medium, chilled, and heat rejection water temperatures and flow rates.

A simplified schematic of the absorption chiller test facility used in this study is provided in Figure 1. The test facility had three main circuits, which independently controlled the chiller inlet temperatures and flow rates. The generator circuit provided the heat input to drive the absorption cycle and the evaporator circuit was where the useful cooling effect occurred. Finally, the condenser/absorber circuit rejected the heat being transferred to the absorption chiller by the evaporator and generator circuits to an externally chilled glycol stream. The test facility included additional measures to ensure boundary conditions at the absorption chiller could be held at steady-state. The functions of the solar thermal collectors, storage tanks, cooling tower and space-cooling load were performed using other hardware in the test facility to carefully control the boundary conditions.

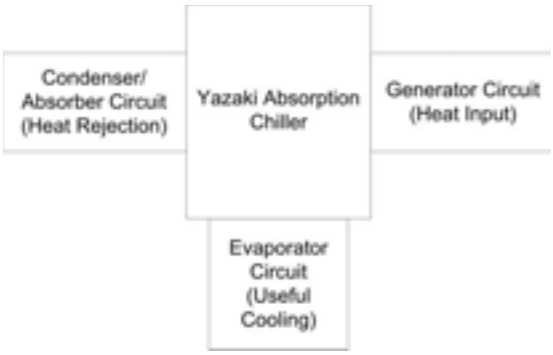

Figure 1: Simplified Schematic of the Absorption Chiller Test Facility

2.1 Experimental Results and Calibration

The experimental results described the inlet and outlet conditions for the generator, evaporator, and condenser/absorber across a range of inlet conditions, described in Table 1. In order to verify the performance characteristics of the absorption chiller test facility, the measured data was compared against manufacturer's performance data (determined by a graphical method). There was general agreement between the manufacturer data and the acquired results; however the operating conditions used in the manufacturer testing were different from the experimental work undertaken.

Table 1: Range of Absorption Chiller Inlet Conditions Tested

	Generator Inlet Temperature (°C)	**Evaporator Inlet Temperature (°C)**	**Condenser/Absorber Inlet Temperature (°C)**
Range Tested	73 - 86	11 - 22	26 - 33

Characteristic equations for the generator and evaporator heat transfer rates were then empirically derived. A linear expression based on the inlet temperature at all three nodes was found to best represent both the generator and evaporator heat transfers. The selected expressions are provided in Equations 1 and 2, where $\dot{Q}$ is the heat transfer rate (kW), T is the temperature (°C), and the subscripts *gen, evap, cond,* and *in* represent the generator, evaporator, condenser, and inlet, respectively. Figure 2 displays the predicted heat transfer rate for each experimental heat transfer result for both the generator and evaporator. The generator heat transfer rate was well predicted, with higher deviations at generator heat transfer rates of 40 kW and higher. The evaporator heat transfer rate was well predicted for all conditions.

$$\dot{Q}_{gen} = -70.387 + 1.9269 * T_{gen,in} + 0.16366 * T_{evap,in} - 1.8824 * T_{cond,in} \text{ (Equation 1)}$$

$$\dot{Q}_{evap} = -46.765 + 1.5296 * T_{gen,in} + 0.08963 * T_{evap,in} - 1.9135 * T_{cond,in} \text{ (Equation 2)}$$

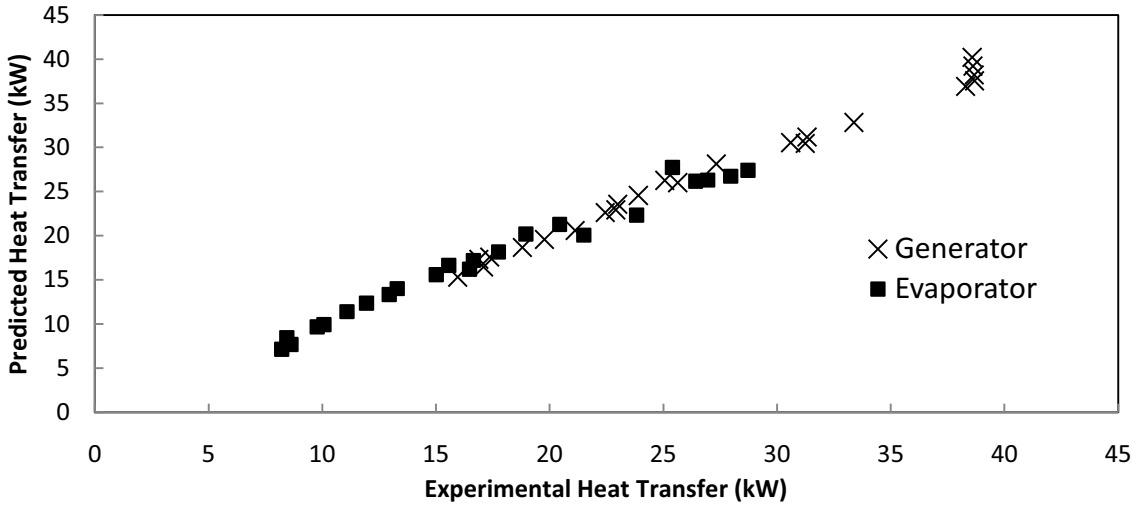

Figure 2: Predicted and Experimental Evaporator and Generator Heat Transfer Rates

3. Solar Absorption Cooling System Setup

After completion of the experimental work, the SAC system was assessed for Ontario housing using building performance simulation (BPS). The SAC simulated is displayed in Figure 3 and was composed of four sub-systems: heat medium production, cold medium production, heat rejection, and load. The heat medium production loop included an array of evacuated tube solar collectors with a 50% glycol solution working fluid, as well as a heat exchanger, a hot storage tank, and circulating pumps. Hot and cold storage tanks were included in order to address the fluctuation in available solar energy. The hot storage tank stored the hot water exiting the solar collector loop heat exchanger and provided the fluid for the inlet to the generator. The cold storage tank stored the chilled water exiting from the evaporator and also provided the chilled water to the load side of the system. The required cooling water streams for the condenser and absorber were connected to a cooling tower.

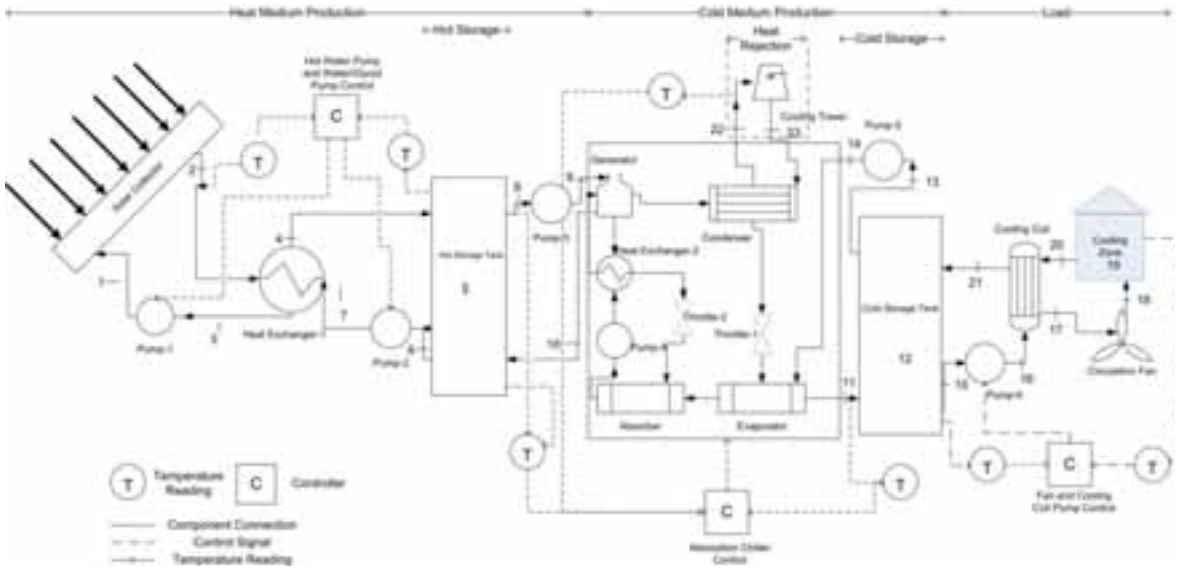

Figure 3: Schematic of the Solar Absorption Cooling System

Once a standardized system design had been selected, building simulation programs were then used to assess the performance of buildings and the related plant networks under a variety of control scenarios. For the initial stages of the present research, BPS software was used to determine the appropriate sizing of a residential SAC system. TRNSYS 17 was selected for the initial sizing of the solar absorption cooling system, due to its ability to rapidly prototype and design, along with the ease in adding and redesigning components. For the overall BPS of houses with the integrated SAC system, a program which utilized a more robust numerical method in finite difference was desired. The ESP-r simulation environment

(ESRU, 2002) utilizes numerical methods for mass and thermal energy balances in the solution of its building and plant networks. Additionally, the ESP-r simulation environment has been extensively validated (e.g. Strachan, 2008) and is an open-source software platform. For this study, ESP-r was selected for the final modelling of the plant network and its integration into Ontario houses with different occupant behaviour strategies and climatic conditions.

3.1 Control Strategies

The SAC system included control strategies for the actuation of the heat production loop, the chiller, and the load loop. For the heat production loop, the actuation of Pump-1 and Pump-2 (Figure 2) were dependent on the availability of solar radiation. Pump-1 and Pump-2 were activated whenever the following two conditions were met: 1) the solar collector fluid temperature was at least 4°C greater than the hot storage temperature; 2) the hot storage tank temperature was less than or equal to 94°C. The latter condition ensured that the hot storage tank was never heated above the maximum generator inlet temperature.

The chiller control strategy actuated Pump-3, Pump-5, and the chiller, based on the chiller inlet conditions. The experimental data was used to provide bounds to the chiller operation, along with the Yazaki guidelines (Aroace, 2010). In order to operate, the chiller required the following conditions to be met:

1. Generator inlet temperature between 73.6°C (experimental) and 95.0°C (Yazaki). If the generator inlet temperature was above 86.6°C (experimental), the heat transfer rate calculations were completed with a generator inlet temperature of 86.6°C.
2. Heat rejection inlet temperature below 32.7°C (experimental). If the heat rejection inlet temperature was below 26.7°C (experimental), the heat transfer rate calculations were completed with a condenser inlet temperature of 26.7°C.
3. Evaporator inlet temperature between 10.8°C and 22.2°C (experimental).

Finally, the control strategy for the zone cooling was based on the zone and cold storage tank temperatures. The zone cooling setpoint was 24 +/- 0.5°C. As long as the cold storage tank temperature was below that of the zone, the fan and pump-6 were actuated once the zone temperature exceeded 24.5°C, and continued to actuate until the zone temperature reached 23.5°C.

3.2 System Component Sizing

TRNSYS 17 was utilized for the initial sizing of the system. The developed system included two custom Types for the modelling of the absorption chiller and the controller. Following the initial sizing, ESP-r was used to complete a more robust sizing using the experimentally obtained chiller data. The final sizing of the components is provided in Table 2. The required solar collector area was determined to be 50 m^2, with combined water tank storage totalling 2.0m^3.

Table 2: Final Sizing of System Components

Variable	Solar Collector Area	Hot Storage Tank Volume	Cold Storage Tank Volume
Final Sizing	50 m^2	0.5 m^3	1.5 m^3

4. Modelling of the Absorption chiller in ESP-r

The performance assessment of the SAC system for houses in Ontario was completed in the ESP-r simulation environment. The ESP-r system developed included a hot loop, a chilled loop, and a load loop. The plant network was composed of existing components from the ESP-r source code, with minor adjustments, and also a novel customized controller component. An existing absorption chiller component was modified for use.

The absorption chiller model in ESP-r was created by Beausoleil-Morrison et al. (2004) and was designed for calibration with experimental data. This model had three nodes: the water-side of the generator, the water-side of the evaporator, and the air-side of the condenser. The model was created to use an experimentally obtained COP_{th} characteristic equation based on the difference between actual and standard conditions for

each node inlet. In order to reduce the number of assumptions and the compounded experimental error from the COP_{th} calculations, the model was modified such that it was based on the experimentally derived relationships for the generator and evaporator heat transfers.

The chiller model was controlled using the custom controller and therefore had no internal control mechanisms. The inlet temperatures, inlet flow rates, and ambient wet bulb temperature were supplied to the chiller component. The condenser inlet temperature, $T_{cond,in}$ (°C), was determined by adding a two degree buffer to the ambient wet bulb temperature ($T_{a,wb}$), as shown in Equation 3. A two degree buffer was assumed to be an appropriate approximation of the local heating effects surrounding the condenser given the structure of the component source code and the nature of the present research (Beausoleil-Morrison et al., 2004).

$$T_{cond,in} = T_{a,wb} + 2 \quad \text{(eq. 3)}$$

After determining the condenser inlet temperature, the chiller model must evaluate the heat transfer that occurs at the generator and evaporator. The generator and evaporator heat transfer rates were determined through the experimentally derived equations described by Equations 1 and 2.

Once the heat transfer occurring at the evaporator and at the generator had been determined, an energy balance was completed on the chiller as a whole. The resulting condenser heat transfer, $\dot{Q}_{con}$ (kW), was determined using Equation 4, where P_{aux} (kW) is the user-specified auxiliary pump power.

$\dot{Q}_{cond} = \dot{Q}_{gen} + \dot{Q}_{evap} + P_{aux}$ (Equation 4)

The thermal coefficient of performance was calculated using Equation 5.

$COP_{th} = \frac{\dot{Q}_{evap}}{\dot{Q}_{gen}}$ (Equation 5)

The matrix equation for each of the nodes was then described for the simultaneous solution of the outlet nodal temperatures of the chiller along with the remaining plant components, based on a simple nodal energy balance of the form shown in Equation 6.

$\dot{Q} = \dot{m}C_p(T_{outlet} - T_{inlet})$ (Equation 6)

5. Modelling of Ontario Houses

In order to accurately assess the performance of the SAC system in Ontario houses, a number of house models were utilized. Swan et al. (2009) developed a database of representative houses across Canada, called the Canadian Stock of Single-Detached, Double, and Row Houses Database (CSSDRD). The house models include a high level of detail, including required inputs for full thermal analysis in ESP-r simulations. From this database (over 16,000 houses), four house models were selected for use in the present research, which represented a number of vintages, construction materials, storeys, and window areas.

The base case house is shown in Figure 4. The main zone (main_1) received all of the cooling, while the second main living zone (main_2), received cooling by means of inter-zone air flow. Each of the houses incorporated internal gains from appliances and lighting, as well as air exchange with the exterior through cracks and gaps. The base climate for the assessment of the SAC system was the Canadian Weather for Energy Calculations (CWEC) Toronto (Numerical Logics, 1999) weather file. The CWEC files are derived from hourly weather information for Canada from 1953-1995. They are representative of conditions which would result in average cooling loads in buildings, based on statistically comparing various climatic conditions (Environment Canada, 2011).

The system was simulated with the base case house in three different Ontario municipalities: Greater Toronto Area (GTA), Windsor, and Ottawa. These three populated cities have relatively high summer temperatures for the Ontario region, with average ambient temperatures between 18°C and 20°C. The number of hours with ambient temperatures above 30°C for the cities is in the range of 20-31 hours. It was assumed that the design of the GTA houses was representative of urban Ontario houses and that they were appropriate for testing in the Windsor and Ottawa municipalities.

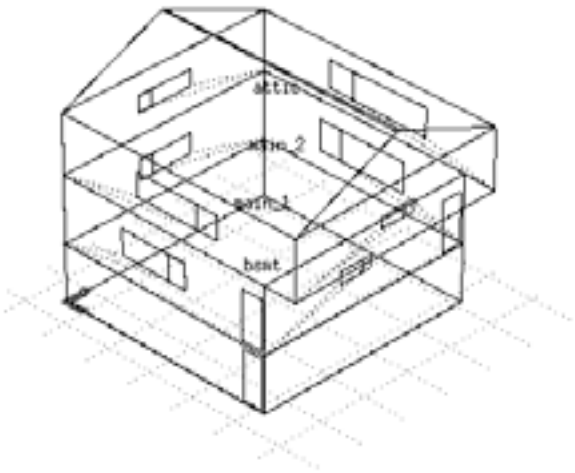

Figure 4: Wireframe Diagram of Base Case House Model

The base case house model was also simulated with the Toronto Pearson International Airport CWEEDS data from 1999 to 2008 in order to assess the ability of the system to meet cooling loads across the temporal variance of an individual city.

6. Results

The cooling season investigated ranged from May 15 to September 15. The parameter Ɲ, described by Equation 7, was used for the determination of the performance of the system, where n is the number of zones. To begin, the base case system was simulated. The summary of results for the base case is presented in Table 3.

$$Ɲ = \frac{\sum_{i=1}^{n} Number\ of\ timesteps\ zone\ temperature\ above\ 25°C}{Number\ of\ timesteps * n} * 100 \quad \text{(Equation 7)}$$

Table 3: Summary of Results for the Base Case Model

Climate	Avg. Ambient Temp. (°C)	Number Hours Ambient Temp. Above 30°C	Ɲ(%)	Max. Zone Temp. (°C)	Avg. Zone Temp. (°C)
Toronto CWEC	18.3	31	2.5	27.2	23.4

The temperature trends for the zone temperature, ambient temperature, and available solar radiation on a typical day (July 4th) are shown in Figure 5. The morning hours serve as a time to charge the hot tank to the maximum generator operating temperature. The chiller activates throughout the day, with more frequent activations in the afternoon and evening hours. The zone temperature fluctuates between 23.5°C and 24.5°C, corresponding to the cooling deadband.

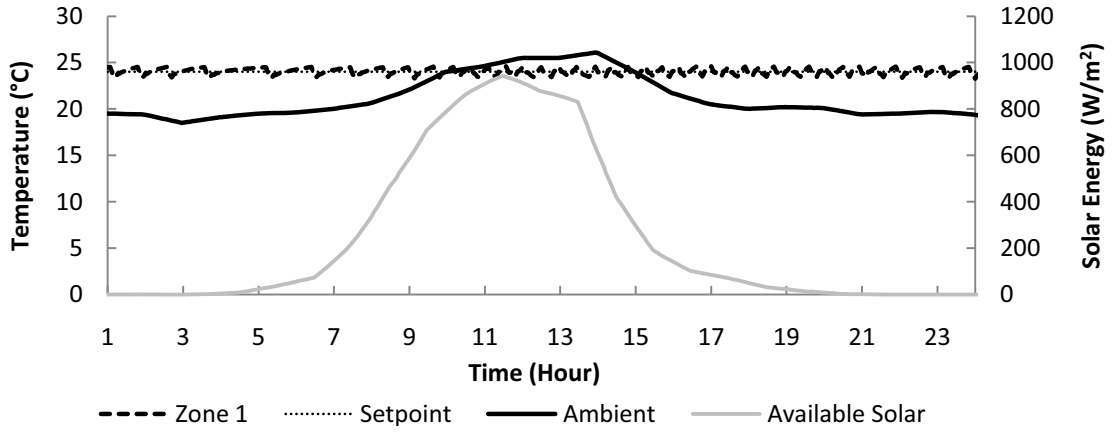

Figure 5: Zone and Ambient Temperatures on July 4th

A similar plot is shown for the day with the peak zone temperature, August 4th, in Figure 6. The ambient temperature on August 4th was in a similar range as that of July 4th, but the solar radiation was significantly lower. This low radiation resulted in the hot storage tank being unable to maintain the minimum generator inlet temperature. Once the tank reached the minimum generator inlet temperature, the chiller immediately activated, drawing the hot storage tank temperature down and consequently cycling the chiller off. The hot storage tank then recharged until it reached the setpoint and again the chiller activated immediately. As a result of the low solar radiation, the hot tank could no longer be charged and the chiller remained inactive by hour 15. This inactivity resulted in a steadily increasing cold tank temperature, and consequentially a steadily increasing zone temperature. Zone 1 reached a peak temperature of 27.2°C in the late evening.

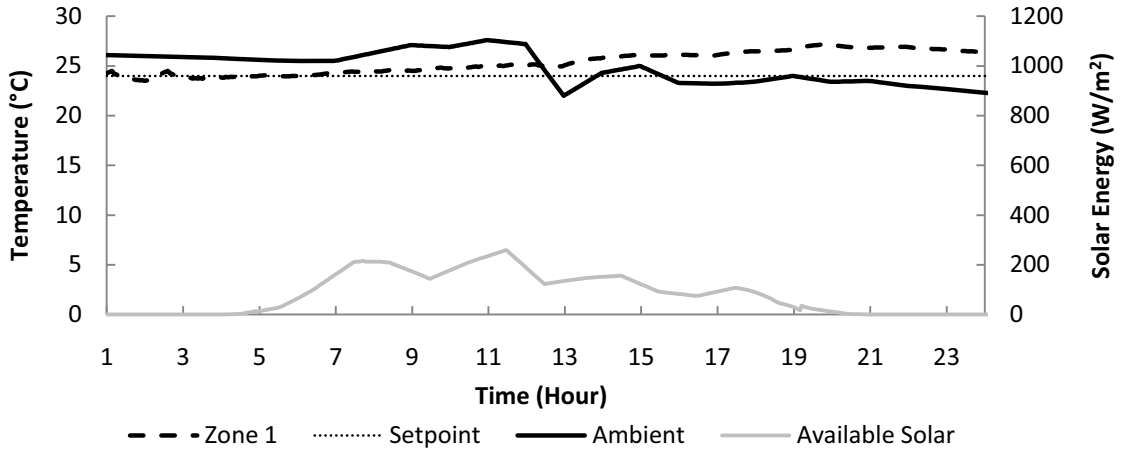

Figure 6: Zone and Ambient Temperatures on August 4th

The energy flow for a typical day, July 4th, is shown in Figure 7. The available solar energy for the day is 1050.9 MJ, only about 22% of which is absorbed for use in the SAC system due to sporadic solar collector pump activation and solar collector inefficiencies. The resultant energy is available to the generator, along with 27.8 MJ from the hot storage tank, which allows 189.4 MJ of energy to be removed through the evaporator. The resulting cooling output is 184.7 MJ, along with 0.5 MJ of additional storage in the cold tank. The diagram shows the heat loss in the hot storage tank and heat gain in the cold storage tank, as well as the auxiliary power input. The major loss of available solar energy occurs from the sporadic activation of the solar collector loop and the coefficient of performance of the chiller.

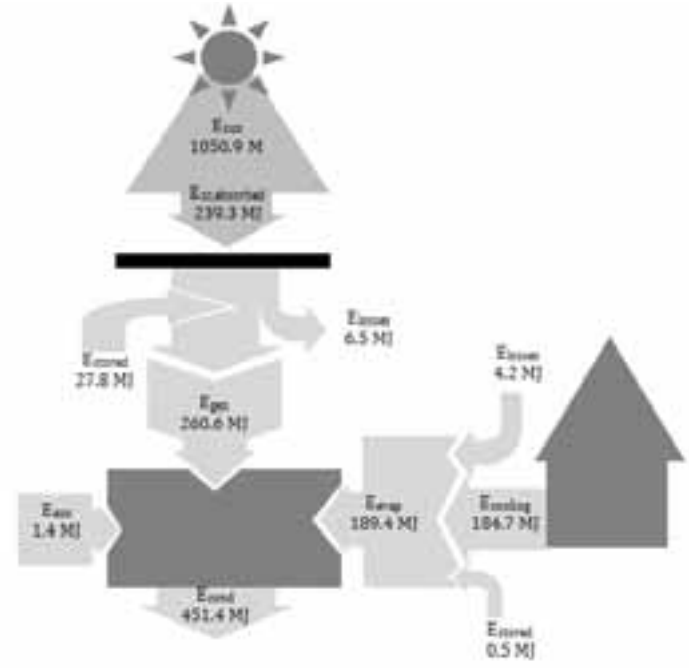

Figure 7: System Energy Flow on July 4th

The overall monthly performance of the chiller is shown in Table 4. The parameter definitions are provided in Equations 8 through 13.

$Q_{captured}(MJ) =$ solar energy capatured by solar collector (Equation 8)

$Q_{avail_{on}}(MJ) =$ incident solar energy on collector at timesteps when solar collector loop is activated (Equation 9)

$$COP_{th} = \frac{Q_{evap}}{Q_{gen}} \text{ (Equation 10)}$$

$$COP_{elec-chiller} = \frac{Q_{evap}}{P_{elec-chiller}} \text{ (Equation 11)}$$

$$SF_{system} = \frac{Q_{cooling}}{Q_{avail_{on}}} \text{ (Equation 12)}$$

$$COP_{elec-system} = \frac{Q_{cooling}}{P_{elec-system}} \text{ (Equation 13)}$$

The average daily cooling was found to be 86 MJ/day, with a maximum daily average cooling of 139 MJ/day occurring in July. The chiller was able to meet all of the loads in May, June, and September, while the system was unable to maintain the setpoint for a portion of both July and August. A significant finding is the number of days where temperatures above the setpoint occur – only three sequential days in each July and August. This suggests that while the chiller failed to maintain the cooling setpoint 2.5% of the timesteps, this was concentrated over only a few days.

In August, the three sequential days of unmet cooling loads began on August 4th, shown earlier. This day of low solar radiation resulted in the peak zone temperature and caused a lasting effect for another 36 hours.

The COP_{th} of the chiller was fairly consistent throughout the summer, with a maximum monthly average of 0.74 in May. The chiller activated less frequently in May, resulting in higher generator inlet temperatures, which improved the chiller performance. The chiller was in operation 114 out of the 124 days simulated, with daily operation occurring in August.

Table 4: Monthly System Performance Parameters

	May	June	July	Aug.	Sept.	Total
Incident Solar Energy (MJ)	18660	33252	34220	30599	12984	129715
$Q_{captured}$ (MJ)	233	2870	6194	5035	1321	15653
Cooling Energy (MJ)	95	1955	4181	3419	838	10488
Average Daily Cooling (MJ/day)	11	70	139	110	70	85
N (%)	0.0	0.0	3.5	5.8	0.0	2.5
Days with unmet cooling loads	0	0	3	3	0	6
COP_{th}	0.74	0.72	0.69	0.70	0.73	0.70
$COP_{elec-chiller}$	169	149	106	110	148	117
SF_{system}	0.09	0.21	0.24	0.22	0.20	0.20
$COP_{elec-system}$	6.9	9.3	8.0	7.7	9.1	8.2
Days Chiller in Operation/Days Simulated	9/17	28/30	30/31	31/31	12/15	110/124

6.1 Climatic Considerations

Following the base case simulation, the SAC system was simulated in different Ontario climates. The results for the system simulation in Windsor and Ottawa were consistent with the Toronto results. The average zone temperature and number of timesteps with unmet cooling loads were unvarying in all three cases, while the maximum zone temperature showed some minor variations. Figure 8 shows the maximum monthly Zone 1 temperature for the base case house for each climate. The width of each slice represents the number of days simulated in that month. The radius of each circle represents the maximum zone temperature, with the centre

of each circle representing 19°C, and each consecutive circle representing an additional degree. The maximum monthly Zone 1 temperatures occurring in each climate were found to be similar, with a slightly higher peak in Toronto in August, and a significant peak of 28.2°C in July in Ottawa. This maximal temperature corresponds to July 20th, the climax of a hot week in Ottawa. Further details of the climatic results can be found in Edwards (2011).

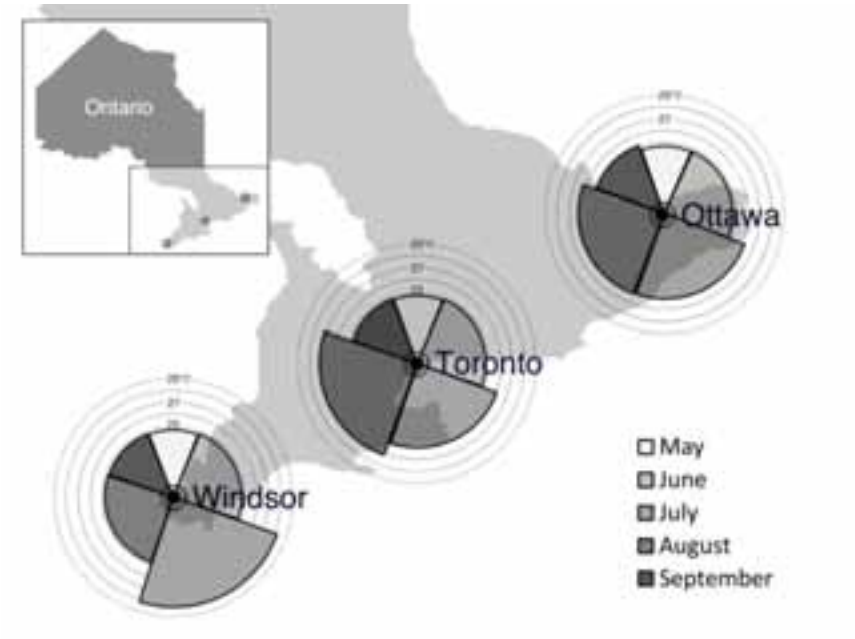

Figure 8: Maximum Monthly Zone Temperature for each Climate Region

Given the variation of temperatures and humidity of a particular climate each year, the performance of the SAC system in the base case house was modelled from 1999 to 2008 in the Toronto region using CWEEDS weather files. Figure 9 shows the resulting percentage of unmet cooling loads for each summer, as well as the maximum occurring and average temperatures for Zone 1. Table 5 displays weather information about each of the years. The hot summers of 2002 and 2005 in Toronto resulted in the highest frequency of zone temperatures above the setpoint of 24°C, but the highest peak zone temperature occurred in 2006.

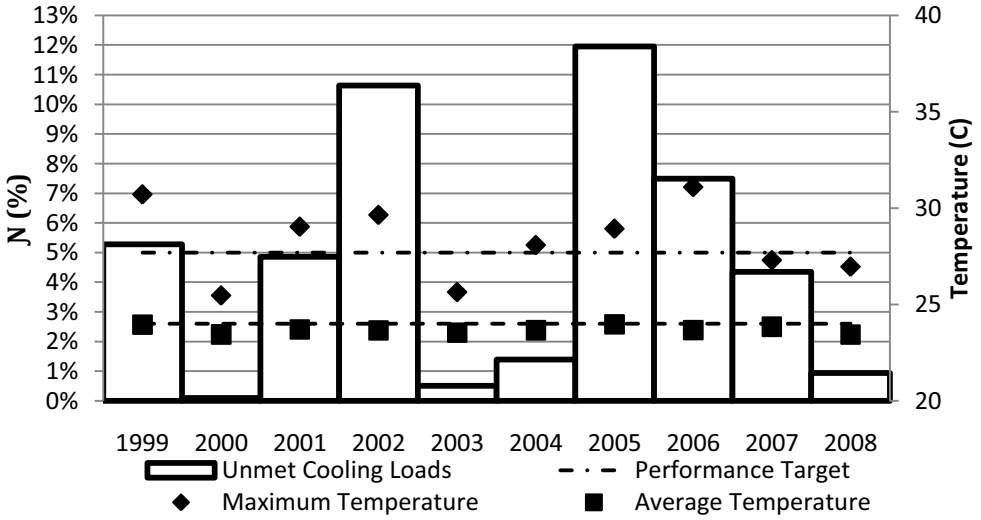

Figure 9: Unmet Cooling Loads and Maximum and Average Zone Temperatures in Toronto from 1999-2008

The SAC system was able to meet the cooling loads and maintain the desired comfort conditions at least 95% of the time for six of the summers investigated. The remaining four summers had over-heated living zones between 5.3% and 12.0% of the time. The decade-long simulations show that while changes in weather do not affect the average zone temperature, they do significantly affect the peak temperature and frequency of peak temperatures.

Table 5: Summary of Weather and Performance Variables for Toronto Pearson International Airport for 1999-2008

Year	1999	2000	2001	2002	2003	2004	2005	2006	2007	2008
Avg. Ambient Temp. (°C)	20.9	18.5	20	20.7	19.5	18.6	21.5	20.1	20.5	19
Avg. Daytime Global Horizontal Solar Radiation (W/m^2)	392.2	355.5	401.7	419.8	387.9	353.4	404.8	354	397.2	358.2
Number of Hours $T_{amb} > 30°C$	123	6	107	188	65	8	159	105	124	25
Number of Hours $T_{amb} > 30°C$ and Radiation < 500 W/m^2	4	0	3	2	0	0	3	4	1	0
N (%)	5.3	0.1	4.9	10.6	0.5	1.4	12.0	7.5	4.3	0.9
Max. Zone Temp. (°C)	30.7	25.5	29	29.6	25.6	28.1	28.9	31.1	27.3	27
Avg. Zone Temp. (°C)	23.9	23.4	23.7	23.6	23.5	23.7	24	23.7	23.8	23.4

Comparing N in Table 5 shows that the peak number of unmet cooling loads coincides with the years with the highest number of hours with high ambient temperatures and low solar radiation. While these occurrences don't account for all unmet cooling loads, it does affirm the finding that the system performs most poorly on hot days with low solar radiation. This finding also explains the higher number of unmet cooling loads in 2006, despite the higher average ambient temperature and solar radiation in 2007.

The system was also simulated with a variety of cooling setpoints, generator inlet temperatures, and house designs. The system was robust enough to successfully maintain a lower cooling setpoint of 23 +/- 0.5°C. Higher generator inlet temperatures were found to decrease the maximum zone temperature and mildly reduce the number of timesteps with unmet cooling loads. The system failed to meet the cooling setpoint on days with high temperatures and low incident solar radiation, and in houses with particularly high window areas and high associated solar gains.

7. Greenhouse Gas Emissions Analysis

One of the primary motivations for the use of solar absorption cooling is to reduce the peak load on the electrical grid during the summer months. Peak loads are supplied by greenhouse gas (GHG) intensive energy generation sources, and therefore a decrease in peak loads would result in a decrease in GHG emissions. The performance of the base case house was simulated both with the inclusion of the SAC system and with an ideal model of a vapour-compression cooling system in ESP-r. The electrical consumption of each case was compared, and the resulting reduction in GHG emissions of the SAC system was determined using Farhat & Ugursal (2010).

The breakdown of electricity generation by source in Ontario is nuclear (50%), hydro (21%), coal (18%), natural gas (8%), and wind (1%) (Farhat & Ugursal, 2010). For simplicity, wind, hydro, and nuclear generators are not considered to have any greenhouse gas emissions. The GHG emission reduction was determined by comparing the electrical consumption of the base case house (Swan et al., 2009) modelled with the vapour-compression system and the solar absorption cooling system.

Once the reduction in electricity consumption for the base case house with Toronto CWEC climate was

determined with the implementation of the SAC system, the GHG emission reduction was calculated. Table 6 provides the monthly reduction in electricity consumption of the SAC system relative to the traditional vapour-compression system and the resulting GHG emission reduction. The total GHG emissions of the house's cooling system were reduced by 614 kg CO_{2e}.

Table 6: Monthly Greenhouse Gas Emission Reduction

Month	Reduction in On-Site Electricity Consumption (MJ)	GHG Emission Reduction ($kgCO_{2e}$)
May	95.3	14
June	856.3	130
July	1527.7	221
August	1360.2	197
September	389.7	52
Total	4229.2	614

The average Canadian was responsible for 22.04 tonnes of CO_{2e} in 2008, with 1.3 tonnes from residential sources (Environment Canada, 2010). The implementation of a SAC system for a household of four would account for an approximate reduction of 12% of the household's annual residential GHG emissions. These results demonstrate that SAC is not only feasible in Ontario, but also would provide much needed relief from peak electrical grid loading and provincial GHG emissions.

8. Conclusions

Residential space-cooling accounts for a significant level of electricity use during the summer months in Canada. Solar absorption cooling reduces the electrical draw from space-cooling and positively impacts the electricity grid during the peak summer season in Ontario. The reduction in electrical draw consequently reduces emissions from greenhouse gas-intensive peak demand energy sources.

The assessment of the suitability of SAC as an alternative to traditional vapour compression cooling was undertaken for Ontario residences using experimental testing of a small-scale absorption chiller. The research objectives were to create an accurate model of a full, appropriately-sized solar absorption cooling system for use in building performance simulation software. The system was designed and first sized using TRNSYS 17 software and later implemented in a full building model in the ESP-r simulation environment. The performance of the system was assessed within different house geometries, operating conditions, and climatic regions. The system was found to perform well with a large solar collector area of 50 m^2, and two water storage tanks totalling 2.0 m^3.

The electrical draw for the SAC system was significantly lower than a vapour compression system, resulting in a substantial reduction in greenhouse gas emissions. These results affirmed the feasibility and environmental benefits of using a solar absorption cooling system for space-cooling in Ontario.

The results of the research attest to the potential use for solar absorption cooling in Ontario climates, while also providing motivation for further research into the application of residential SAC systems and the associated barriers to adoption.

9. Acknowledgements

The authors are grateful for the funding provided by the Natural Sciences and Engineering Research Council of Canada through the Alexander Graham Bell Canada Graduate Scholarship, and the Solar Buildings Research Network.

11. References

Aroace. (2010). *Water Fired Single-Effect Absorption Chiller and Chille-Heater.* Plano Texas: Yazaki Energy Systems, Inc.

Balaras, C., Grossman, G., Henning, H.-M., Infante Ferreira, C., Podesser, E., Wang, L., et al. (2007). Solar air conditioning in Europe - an overview. *Renewable & Sustainable Energy Reviews* , 299-314.

Balghouthi, M., Chahbani, M., & Guizani, A. (2005). Solar Powered air conditioning as a solution to reduce environmental pollution in Tunisia. *Desalination* , 105-110.

Beausoleil-Morrison, I., Mottillo, M., Brandon, R., Sears, P., & Ferguson, A. (2004). The Simulation of a Residential Space-Cooling System Powered by the Thermal Output of a Cogeneration Device. *ESim - The Canadian Conference on Building Energy Simulation* (p. 163). Vancouver: IBPSA-Canada.

Edwards, C. (2011). *Performance Assessment of Solar Absorption Cooling for Ontario Housing.* Ottawa: Carleton University.

Environment Canada. (2010, 11 9). *Greenhouse Gas Emissions Data*. Retrieved 06 20, 2011, from Environment Canada: http://www.ec.gc.ca/indicateurs-indicators/default.asp?lang=en&n=BFB1B398-1#ghg7_en

Environment Canada. (2011, May 18). *National Climate Data and Information Archive*. Retrieved 06 17, 2011, from Environment Canada: http://climate.weatheroffice.gc.ca/prods_servs/index_e.html

ESRU. (2002). *The ESP-r system for building energy simulation: user guide version 10 series.* Retrieved from Energy Systems Research Unit: www.esru.strath.ac.uk

Farhat, A. A., & Ugursal, V. I. (2010). Greenhouse gas emission intensity factors for marginal electricity generation in Canada. *International Journal of Energy Research* , 1309-1327.

Henning, H.-M. (2007). Solar assisted air conditioning of buildings – an overview. *Applied Thermal Engineering* , 1734-1749.

Johnson, G. (2011). *Design and Commissioning of an Experiment to Characterize the Performance of a Lithium-Bromide Absorption Chiller.* Ottawa: Carleton University.

Mateus, R., & Oliviera, A. (2009). Energy and Economic Analysis of an Integrated Solar Absorption Cooling and Heating System in Different Building Types and Climates. *Applied Energy , 86* (6), 949-957.

NRCan. (2008). *Natural Resources Canada.* Retrieved 09 20, 2009, from Economic Scan of Canada's Energy Sector: Residential Sector: http://www.sst.gc.ca/default.asp?lang=En&n=AADC6287-1&offset=3&toc=show

Numerical Logics. (1999). Canadian Weather for Energy Calculations, Users Manual and CD-ROM. Downsview, Ontario: Environment Canada.

Swan, L., Ugursal, V., & Beausoleil-Morrison, I. (2009). A database of house descriptions representative of the Canadian housing stock for coupling to building energy performance simulation. *Journal of Building Performance Simulation , 2* (2), 75-84.

Zhai, X. Q., & Wang, R. Z. (2009). A review for absorbtion and adsorbtion solar cooling systems in China. *Renewable and Sustainable Energy Reviews* , 1523-1531.